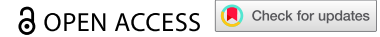Taylor & Francis
Taylor & Francis Group

RESEARCH PAPER

GRP75 as a functional element of cholix transcytosis

Keyi Liu[a], Tom Hunter[a], Alistair Taverner [ID][b], Kevin Yin[a], Julia MacKay[b], Kate Colebrook[a], Morgan Correia[a], Amandine Rapp[a], and Randall J. Mrsny [ID][a,b]

[a]Applied Molecular Transport, South San Francisco, CA, USA; [b]Department of Pharmacy and Pharmacology, University of Bath, Bath, UK

ABSTRACT

Cholix (Chx) is secreted by non-pandemic strains of *Vibrio cholerae* in the intestinal lumen. For this exotoxin to induce cell death in non-polarized cells in the intestinal lamina propria, it must traverse the epithelium in the fully intact form. We identified host cell elements in polarized enterocytes associated with Chx endocytosis and apical to basal (A→B) vesicular transcytosis. This pathway overcomes endogenous mechanisms of apical vesicle recycling and lysosomal targeting by interacting with several host cell proteins that include the 75 kDa glucose-regulated protein (GRP75). Apical endocytosis of Chx appears to involve the single membrane spanning protein TMEM132A, and interaction with furin before it engages GRP75 in apical vesicular structures. Sorting within these apical vesicles results in Chx being trafficked to the basal region of cells in association with the Lectin, Mannose Binding 1 protein LMAN1. In this location, Chx interacts with the basement membrane-specific heparan sulfate proteoglycan perlecan in recycling endosomes prior to its release from this basal vesicular compartment to enter the underlying lamina propria. While the furin and LMAN1 elements of this Chx transcytosis pathway undergo cellular redistribution that are reflective of the polarity shifts noted for coatamer complexes COPI and COPII, GRP75 and perlecan fail to show these dramatic rearrangements. Together, these data define essential steps in the A→B transcytosis pathway accessed by Chx to reach the intestinal lamina propria where it can engage and intoxicate certain non-polarized cells.

ONE SENTENCE SUMMARY

The *Vibrio cholerae* exotoxin protein cholix interacts with a number of host cell proteins, including GRP75, to facilitate its vesicular transcytosis across polarized intestinal epithelial cells following apical endocytosis.

Introduction

Bacterial toxins use a variety of pathways to reach the cytosol of target cells where they demonstrate a plethora of actions.[1] Once internalized, often by receptor-mediated endocytosis, these agents modify host component activities that lead to physiological changes to alter cell properties, often resulting in cell death.[2,3] Some toxins incite intestinal pathologies by directly damaging the polarized epithelial cells that line the lumen, altering the robust barrier that functions to restrict the nonspecific uptake of intestinal contents into the body.[4,5] In doing so, a variety of innate and adaptive immune system pathways are triggered that target the pathogen and its associated virulence factors.[6] There are, however, a group of bacterial toxins that appear to first cross the epithelium without damaging these polarized cells and then target underlying cells of

the innate and/or adaptive immune systems. This clandestine epithelial transcytosis with targeted death of selected cells within the *lamina propria* theoretically benefits the establishment of a durable infection at the intestinal lumen. Non-pandemic strains of *Vibrio cholerae* secrete an exotoxin, cholix (Chx), that is capable of translocating through the intestinal barrier to reach the *lamina propria* and which provides an example of this pathophysiological strategy.[7]

Chx is a member of the toxin family that includes the diphtheria toxin produced by *Corynebacterium diphtheriae* and exotoxin A produced by *Pseudomonas aeruginosa*. All three proteins intoxicate mammalian cells by the enzymatic ADP-ribosylation of eukaryotic elongation factor 2 to induce apoptosis through the blockade of protein synthesis.[8,9] The first 266 amino acid (domain I) of

Chx are sufficient for successful completion of apical to basal (A→B) transcytosis across polarized intestinal epithelial cells and targeting of this toxic action to non-polarized cells within the lamina propria.[10] In order to maintain systemic homeostasis and protect the body from toxic elements present in the diet or released by the microbiome, proteins absorbed at the surface of enterocytes via receptor-mediated endocytosis are typically either returned to the intestinal lumen or shuttled to a lysosomal degradation pathway. Since Chx appears to have identified a transcytosis process that avoids these fates,[10] we wanted to better understand the cellular processes that allowed for this unusual outcome.

Examination of Chx function has demonstrated that the capacity for efficient A→B transcytosis lies entirely within domain I of the toxin, including the remarkable capacity of evading the lysosomal degradation pathway following apical endocytosis.[10] Previous studies have identified several proteins that co-localize with Chx at discrete locations within polarized enterocytes and the hypothesis was put forth that sequential interactions with such proteins could provide a mechanism for efficient A→B transcytosis. The term of transient receptor-like proteins (TRIPs) was coined to describe host cell proteins involved in Chx processes of apical endocytosis and vesicular routing across the intestinal epithelium to reach the *lamina propria*. One element of this hypothesis is that mechanisms of Chx engagement with and release from these TRIPs would be transient in nature in order to allow efficient A→B transcytosis to occur. Previous *in vitro* and *in vivo* studies validated the ER intermediate Golgi complex (ERGIC) element LMAN1 (Lectin, Mannose Binding 1) to be one of these TRIPs.[10]

Here we describe additional host cell elements involved in the Chx transcytosis mechanism and correlate their actions in relation to LMAN1 and its redistribution within vesicular structures in response to apical Chx administration. The TRIPs identified include TMEM132A as an apical entry element, the heparan sulfate proteoglycan perlecan that functions in basal release events, furin that engages Chx soon after its endocytosis, and GRP75 that appears to play a role in protecting Chx from a degradative fate. While GRP75 is best known for its functions as a cytoplasmic protein, this protein appears to act as a TRIP for Chx within endosomes. Overall, our studies support the concept that sequential TRIPs are used by Chx to escape targeting to lysosomes and/or recycling to the apical surface following receptor-mediated apical endocytosis; Chx uses interactions with these TRIPs to traffic to the basal region of the cells with subsequent exocytosis to allow access to non-polarized cells within the intestinal lamina propria.

Results

Identification of GRP75 as a Chx interactive protein

An unbiased approach to identify proteins that could interact with Chx during its A→B vesicular transcytosis was performed *in vitro* using polarized monolayers of a human intestinal cell line, Caco-2. A nontoxic form of full-length Chx (ntChx) was prepared where a single amino acid mutation (E581A) in the third domain of the protein abolishes its ADP ribosylation capacity.[9] 100-nm diameter magnetic particles coated with ntChx were used to capture interacting proteins after apical application to polarized Caco-2 cells as previously described.[11] Enrichment of selected proteins compared to a whole cell membrane preparation was verified using 1-D gel electrophoresis (Figure 1a), with a 2-D format (Figure 1b) being used for greater separation. Mass spectrometry-based genome-wide analyses assigned ~45 spots separated by the 2-D method to known human proteins; spot 16 was identified as glucose-regulated protein (GRP)75. Confirmation of GRP75-Chx interaction(s) was achieved using ntChx-magnetic beads to pull down purified recombinant GRP75 using an antibody recognizing human growth hormone (hGH) as a control (Figure 1c). Studies were also performed where Caco-2 cell lysates were first incubated with ntChx with the resulting complexes exposed to magnetic beads decorated with an anti-GRP75 antibody. An anti-GRP75 antibody, but not an isotype control, captured ntChx as detected by Western blot (Figure 1d).
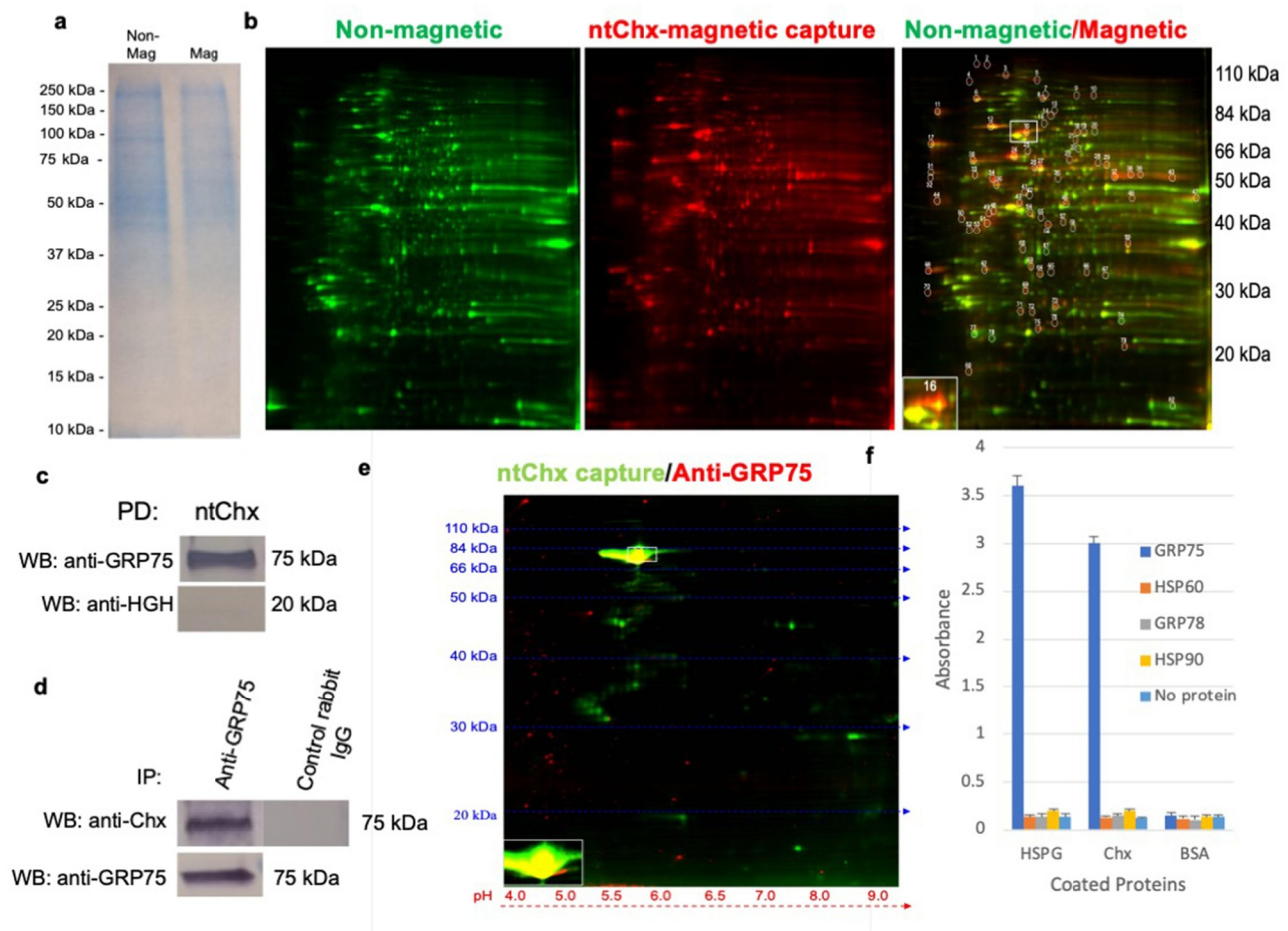
Figure 1. GRP75 is an interactive partner of cholix. Polarized monolayers of Caco-2 cells were exposed apically to nontoxic full-length Chx (ntChx) anchored through a C-terminal hexa-histidine sequence to 100 nm diameter magnetic beads. After 15 min, cell membranes were isolated and separated into non-magnetic and magnetic fractions. a, 1-D SDS-PAGE gel of non-magnetic and magnetic captured membrane fractions. b, 2-D gel separation of proteins present in non-magnetic and magnetic capture membrane fractions with location of spot 16 identified by mass spectrometry as GRP75. c, Pull-down (PD) using ntChx probed with antibodies to either GRP75 or human growth hormone (hGH). d, Immunoprecipitation of Caco-2 cell lysate using ntChx probed with anti-GRP75 or control antibodies. e, 2-D Western blot of magnetic capture membrane fraction probed with anti-GRP75. f, ELISA-based, neutral pH, format where bound ntChx or the control protein bovine serum albumin (BSA) was used to capture GRP75, heat shock protein 60 (HSP60), glucose-regulated protein 78 (GRP78), or HSP90.

An affinity pulldown of ntChx binding partners from Caco-2 cell lysates was performed using ntChx-magnetic beads, followed by 2-D Western blotting using an anti-GRP75 antibody. One spot interacting with the antibody was observed for an ~75 kDa protein whose position overlapped the bait protein ntChx (Figure 1e). Controls performed for the primary and secondary antibodies demonstrated this interaction to be specific, providing further evidence that GRP75 directly interacts with ntChx. An ELISA-based analysis, performed at neutral pH, was used to examine potential direct interactions of ntChx with other heat shock protein (HSP) family members that have been noted to distribute at the extracellular surface of cellular membranes: HSP60, GRP78, and HSP90 (Figure 1f). Bovine serum albumin (BSA), having a similar molecular weight (66 kDa *vs.* 71 kDa) and isoelectric point (5.0 *vs.* 5.5) to ntChx, was used as a negative control. As a positive control for proteins previously suggested to interact with Chx,[10] perlecan was used as the capture protein. Here, perlecan was found to interact with GRP75 but not HSP60, GRP78, or HSP90 (Figure 1f). These data support direct interaction events between GRP75 and ntChx that reflect specific exotoxin interactions

following an uptake into intracellular vesicles and suggest a direct interaction between GRP75 and perlecan.

GRP75 and perlecan are involved in Chx transcytosis

From the mass spectrometry-based genome-wide analyses, we identified heparan sulfate proteoglycan family member perlecan and cytokeratin 8 (CK-8), along with GRP75, as potential TRIPs for Chx. Of note, CK-8 has been identified as the epithelial cell receptor for the cytotoxic serine protease toxin Pet[12] and perlecan was previously shown to co-localize with ntChx during A→B transcytosis.[10] We assessed the potential role of these proteins in Chx A→B transcytosis by gene knockdown of *HSPA9* (GRP75), *HSPG2* (perlecan), or *KRT8* (cytokeratin 8) using a CRISPR-Cas9 strategy in Caco-2 cells. Stably modified Caco-2 cells were observed to have ~15–20% reduction in protein expression from this knockdown protocol for all three targets (Supplemental Figure 1). This level of knockdown allowed these cells to retain the capacity to form polarized monolayers, verified by the establishment of trans-epithelial electrical resistance (Supplemental Table 1), that was required for comparison of Chx transcytosis properties relative to parent Caco-2 cells. This low level of knockdown must be cautiously interpreted due to the possibility of off-target effects. Nonetheless, Chx A→B transcytosis was examined over a 60 min timeframe using Chx266-hGH, a chimeric protein of ~50kDa composed of the first 266 amino acids (domain I) of Chx genetically fused to human growth hormone (hGH) as previously described; nonselective paracellular leak across these monolayers was evaluated using a molar equivalent of apically added hGH.[10] Chx266-hGH A→B transcytosis, which dramatically out-paced the rate of nonselective hGH leak, was similar for the parent Caco-2 cell-line CK-8 knockdown (Figure 2a). Similar studies using polarized monolayers established with GRP75 knockdown cells, however, showed suppressed Chx266-hGH transcytosis without affecting nonselective hGH leak (Figure 2b). Reduction in Chx266-hGH transcytosis was also observed using monolayers established with perlecan knockdown Caco-2 cells (Figure 2c). Comparison of densitometry ratios demonstrated a reduction in Chx266-hGH

A→B transcytosis relative to hGH leak for Caco-2 monolayers with reduced expression of GRP75 and perlecan proteins but not CK-8. Finally, addition of an antibody recognizing either GRP75 or perlecan, but not an isotype control against human interleukin 10 (IL-10), to the apical compartment of Caco-2 monolayers suppressed A→B Chx266-hGH transcytosis (Figure 2d). Thus, despite an incomplete protein knockdown, modest reduction in the cellular levels of GRP75 or perlecan expression resulted in diminished Chx A→B transcytosis.

TMEM132A is associated with Chx during its apical endocytosis

We next examined the cellular distribution of GRP75 in relation to potential endocytosis and early trafficking events for Chx, as GRP75 has been shown to participate in the endocytosis induced by heparan binding proteoglycans in non-polarized cells.[11] These studies were performed in association with TMEM132A, a putative TRIP identified through the ntChx-magnetic bead capture of GRP78. TMEM132A, also known as GRP78-binding protein 1,[13] is a single-pass type I transmembrane protein that contains a cytoplasmic (N-terminal) self-association element[14] and an extracellular cohesin domain that appears to function in protein–protein interactions.[15] While we were unable to validate an involvement for GRP78 in Chx A→B transcytosis and ntChx failed to interact directly with GRP78 at neutral pH (Figure 1f), sequence similarities between GRP75 and GRP78 prompted us to test the potential role of TMEM132A in Chx apical endocytosis. For these *in vivo* studies we followed AMT-101, a genetic fusion protein composed of Chx386 and human interleukin-10.[16]

At 1 min post-intraluminal injection (ILI) of AMT-101 into rat jejunum *in vivo*, TMEM132A and AMT-101 (observed as hIL-10) were co-localized in microvilli, being particularly focused at or near the base of these structures (Figure 3a). TMEM132A, but not AMT-101, was observed in the narrow band region of enterocytes immediately beneath the microvilli, a location consistent with a cytoskeleton-rich region of enterocytes known as the terminal web.[17–19] TMEM132A was restricted in its distribution to microvilli and terminal web regions. Observations of co-localized TMEM132A
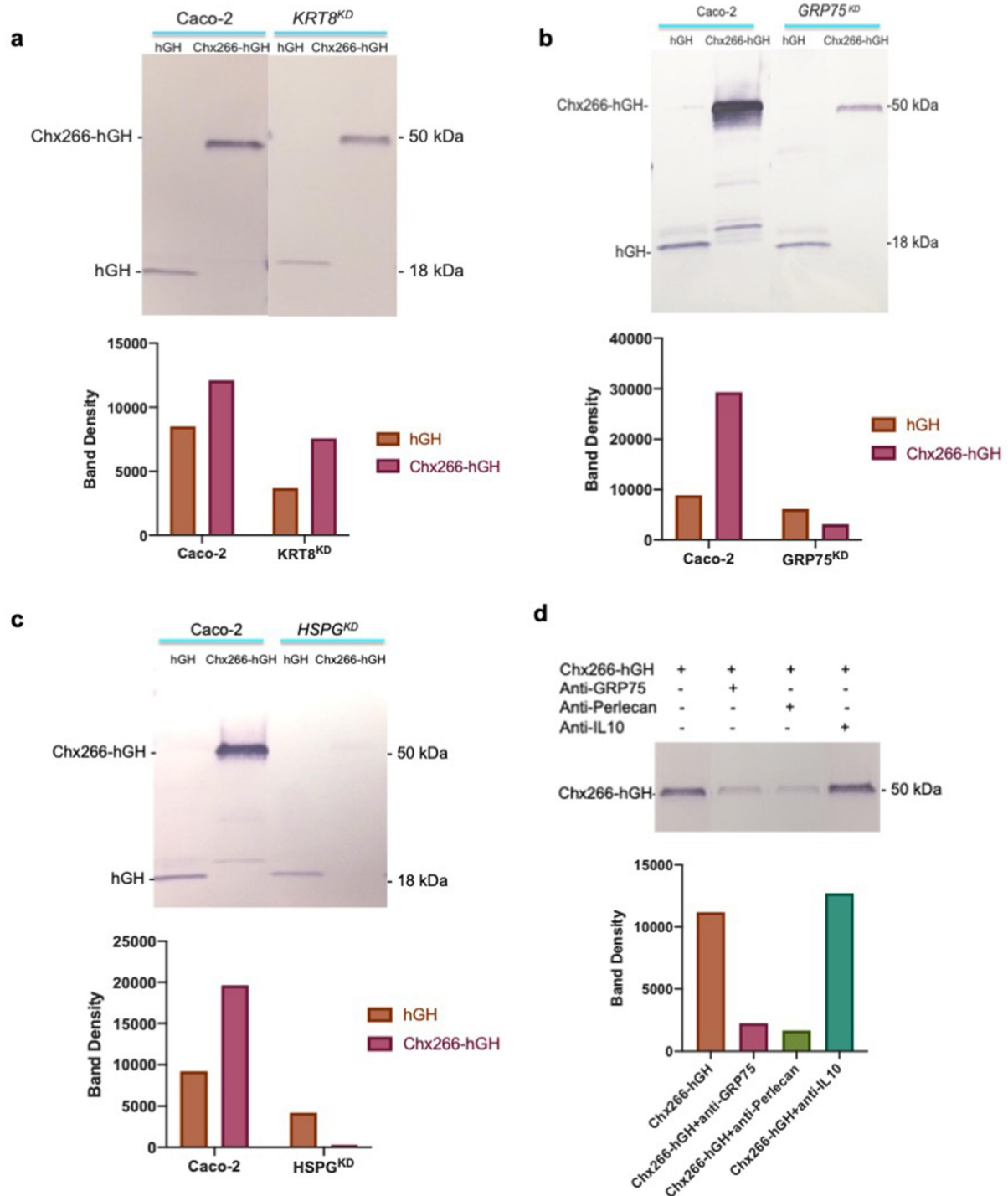
Figure 2. GRP75 and perlecan are functionally involved in cholix transcytosis. Expression of three proteins identified by ntChx-magnetic bead capture were suppressed using a CRISPR/cas 9-mediated knockdown protocol that targeted either *GRP75, HSPG2*, or *KRT8* in Caco-2 cells. Confluent monolayers of the resulting cell lines having decreased levels of a, GRP75, b, perlecan, or c, cytokeratin 8 (CT8) were evaluated for their capacity for Chx-mediated transcytosis using Chx266-hGH and for the nonspecific movement of the control protein hGH over a 60 min time period. d, Transcytosis of Chx266-hGH across confluent monolayers of parent Caco-2 cells was evaluated following a simultaneous apical application of a monoclonal antibody against GRP75 or perlecan, with an isotype antibody recognizing interleukin (IL)-10 serving as a control. Densitometry measurements of individual Western blot bands are shown for graphical comparison.
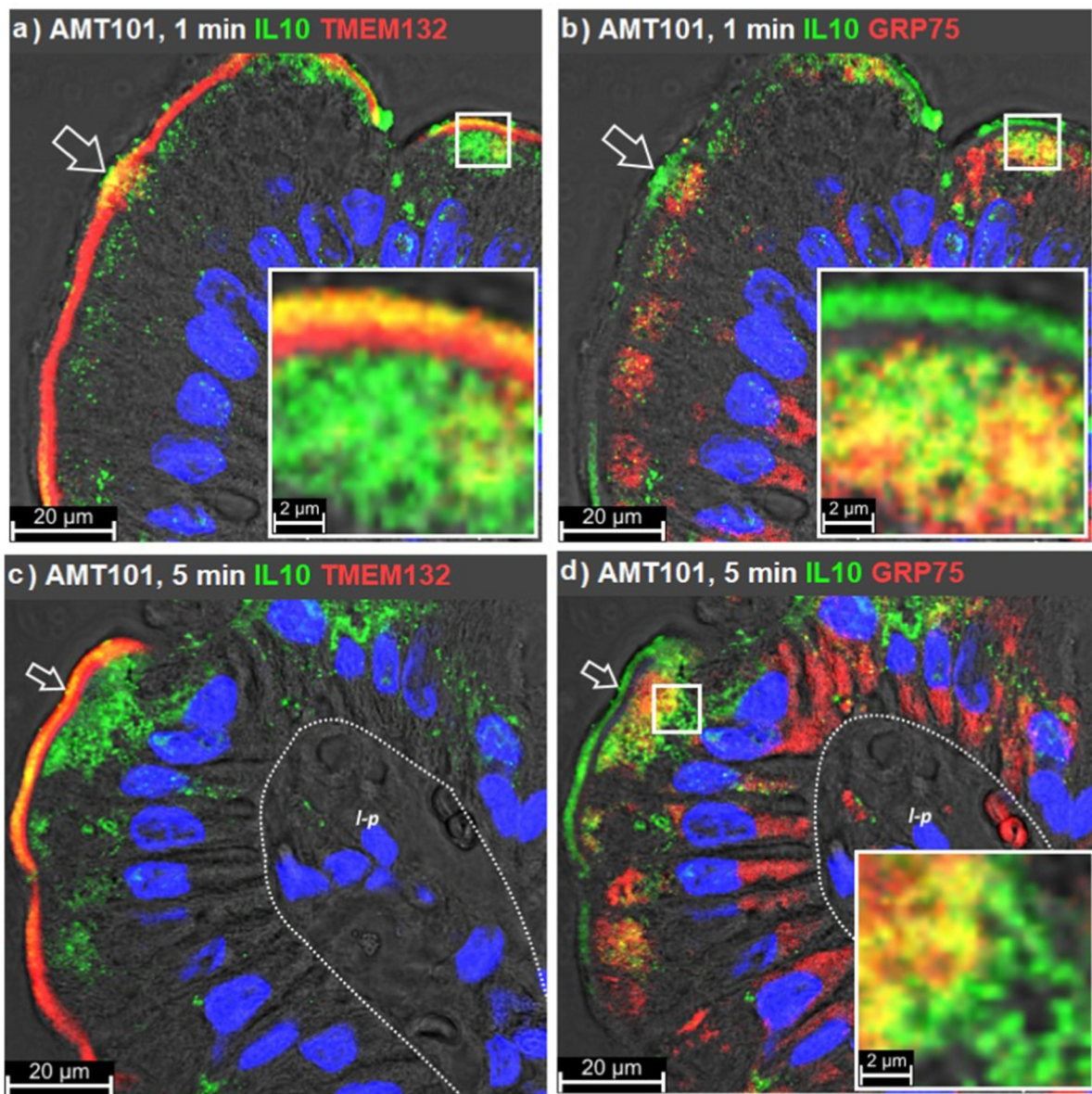
Figure 3. GRP75 associates with cholix in apical endosomes. Immunofluorescence microscopy was performed on rat jejunum over a time course following intraluminal injection (ILI) of AMT-101. Co-localization of the human interleukin (IL)-10 element of AMT-101 with TMEM132A (a, c) or GRP75 (b, d) at 1- or 5-min post ILI. Apical (luminal) epithelial membrane (open arrow); basal epithelial cell surface-basement membrane demarcation (dashed line); *lamina propria* (*l-p*); goblet cell (g). Nuclei were stained with 4',6-diamidino-2-phenylindole (DAPI; blue).

with AMT101 in the terminal web were rare (Figure 3a). While TMEM132A was restricted to microvilli at 1 min post ILI of AMT-101, GRP75 could be seen extensively localized to large areas within the apical and basal regions of enterocytes and to a lesser extent in a supranuclear location (Figure 3b). At 1 min, hIL-10 was detected in GRP75$^+$ vesicles in the apical region of enterocytes just below the terminal web (Figure 3b). By 5 min post ILI of AMT-101, TMEM132A/hIL-10 co-

localizations remained restricted to microvilli with an increased population of hIL-10$^+$/TMEM132A$^-$ vesicles being observed in the apical vesicular region of enterocytes (Figure 3c). At 5 min post ILI, GRP75 was still present in a population of vesicles in the apical and basal vesicular regions and to a lesser extent in a supranuclear region of enterocytes. Of the observed GRP75$^+$ vesicles, only those present in the apical compartment of enterocytes were hIL-10$^+$ (Figure 3d).

While this data supported the role of TMEM132A and GRP75 as TRIPs involved in the apical endocytosis and early vesicular trafficking of Chx, respectively, it did not identify any possible mechanism for transfer of Chx between microvillar and apical vesicular regions and inferred a rapid movement of TMEM132A/Chx through the terminal web to reach the apical vesicular compartment where sorting of the exotoxin to GRP75$^+$ vesicles can occur. To explore this question, we performed ILI studies using Chx266-hGH (observed as hGH)

at the 5 min time point post ILI. As TMEM132A was originally identified as GRP78-binding protein 1, the distribution of TMEM132A and GRP78 in the context of early Chx266-hGH endocytosis and trafficking events was examined. At 5 min post ILI of Chx266-hGH, co-localization with TMEM132A was again observed in microvilli but was now more readily observed in the apical vesicular region (Figure 4a) when compared to studies using AMT-101 (above). At this 5 min time point, GRP78 co-localized with Chx266-hGH (observed
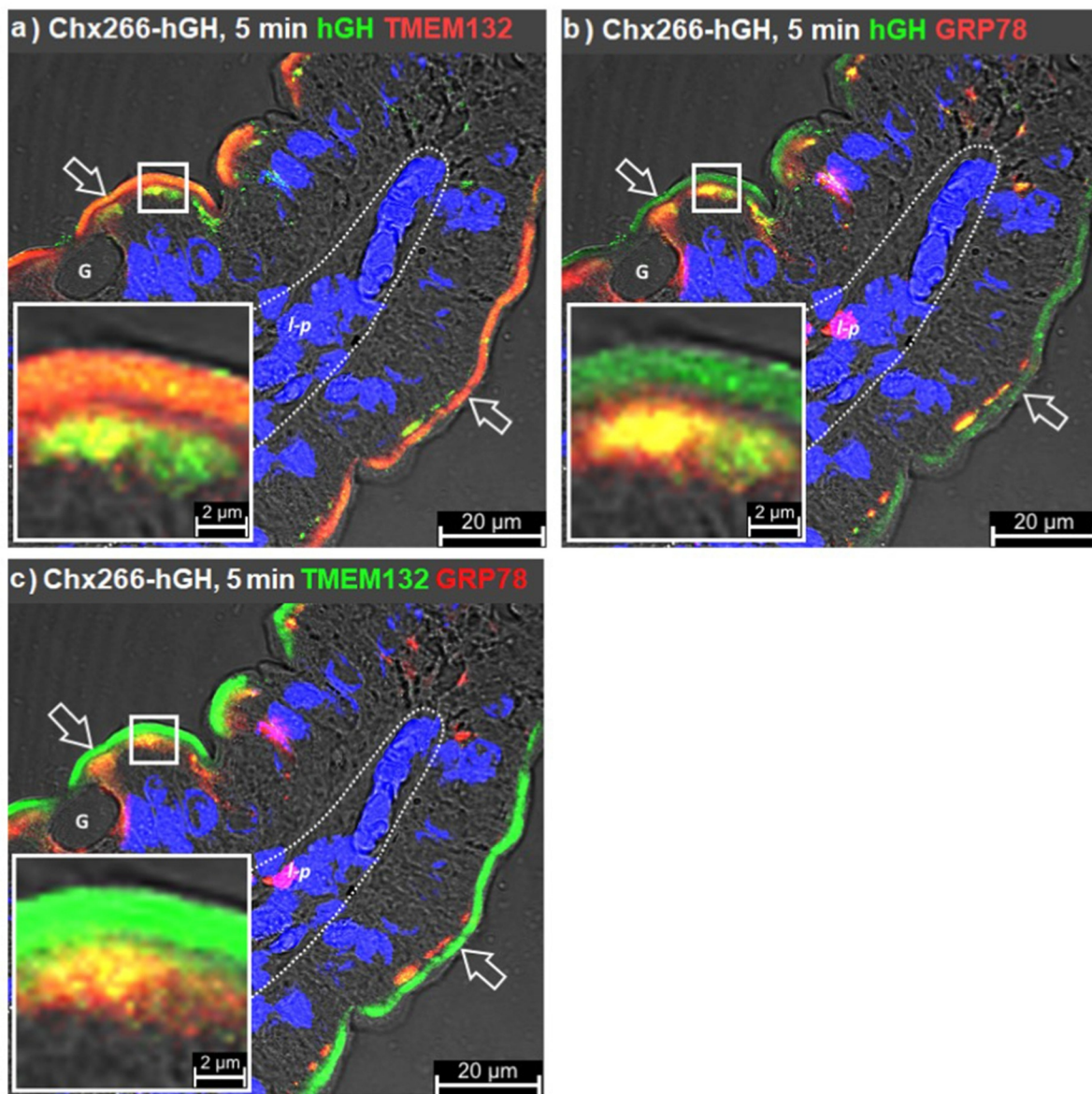
Figure 4. Relationship of GRP75 to GRP78 and TMEM132A. Immunofluorescence microscopy was performed on rat jejunum over a time course following intraluminal injection (ILI) of Chx266-hGH. Co-localization events detecting the human growth hormone (hGH) element of Chx266-hGH with a, TMEM132A or b, GRP78 compared to the co-localization of c, TMEM132A and GRP78 at 5 min post ILI of Chx266-hGH. Apical (luminal) epithelial membrane (open arrow); basal epithelial cell surface-basement membrane demarcation (dashed line); *lamina propria* (*l-p*); goblet cell (g). Nuclei were stained with 4',6-diamidino-2-phenylindole (DAPI; blue).

as hGH) only in the apical vesicular compartment immediately beneath the microvilli layer (Figure 4b). TMEM132A and GRP78 in rat jejunum at 5 min post ILI of Chx266-hGH showed co-localizations that were similarly restricted to the apical vesicular region, but not within the terminal web that separates these two domains (Figure 4c). Strikingly, the distribution of GRP78, and its co-localization with TMEM132A was restricted to the region of the apical vesicular region closest to the terminal web. These results were consistent with the hypothesis that Chx undergoes apical endocytosis and trafficking to the apical vesicular region in vesicles that contain TMEM132A and that within the apical vesicular region, TMEM132A engages with GRP78. TMEM132A/GRP78 co-localizations in the apical vesicular region do not completely describe the Chx distribution, consistent with the hypothesis that Chx moves to a subsequent TRIP, such as GRP75, in this compartment. These findings place GRP75 at a position in Chx A→B transcytosis as a potential acceptor of the toxin soon after apical endocytosis that could function to reduce its trafficking back to the apical surface as TMEM132A recycles to this location.

GRP75 and LMAN1 in early endosomes

Previous studies demonstrated that apical vesicular trafficking events of Chx involved Rab7^{+} vesicles in a manner consistent with sorting to late endosomes but without the subsequent fate of delivery into LAMP1^{+} lysosomes.[10] These results suggested that Chx might associate with at least one element in a post-endocytosis pathway to thwart a destructive fate. We used Chx266-hGH to determine where such a lysosomal pathway deviation might occur by examining endocytosis events involving early endosomal antigen 1 (EEA1), which functions as a tethering protein for early endosome sorting.[20] At 5 min post ILI, EEA1/hGH co-localizations were observed in a subset of vesicles within the apical region of the cell (Figure 5a). EEA1/hGH co-localizations were also observed at a location just basal to the nucleus of enterocytes, but to a lesser extent than that observed in the apical vesicular compartment (Figure 5a). GRP75/hGH co-localizations at 5 min post ILI in the same tissue were highly correlated with EEA1/hGH co-

localizations in this apical vesicular region where hGH[+] vesicles showed distributions of both EEA1 and GRP75 (Figure 5b). Overall, EEA1/hGH co-localizations were noted to be more frequent than GRP75/hGH co-localizations in the supra-nuclear region and sub-nuclear vesicular regions of enterocytes at this 5 min timepoint (Figures 5a,b).

At 15 min post ILI, very little Chx266-hGH was detected in the apical vesicular region; most of the Chx266-hGH observed was in the basal vesicular region of enterocytes and in non-polarized cells within the lamina propria consistent with completion of A→B transcytosis (Figure 5c,d). At this time, most EEA1/hGH co-localizations within enterocytes were observed in the basal vesicular region (Figure 5c), possibly consistent with the recycling compartment containing perlecan that was previously identified as a basal secretion pathway element for Chx.[10] Examination of the same tissue samples showed that these basal EEA1/hGH co-localizations were not GRP75^{+} (Figure 5d). EEA1 and GRP75 were observed in cells within the lamina propria, but these distributions in non-polarized cells did not suggest extensive co-localization (Figure 5c,d). As was observed at the 5 min time point post ILI, EEA1 and GRP75 distribution at 15 min post ILI overlapped extensively within enterocytes, with the exception that EEA1 was now more readily observable within the microvilli of some cells, but without GRP75 co-localization (Figure 5c,d). We hypothesize that the difference in apparent distribution of EEA1 within microvilli at 5 and 15 min reflects a very short residence time during the highly active receptor-mediated uptake of Chx266-hGH that engages EEA1 movement from the microvilli to the apical vesicular region that subsides over time after ILI.

We next examined the relationship of EEA1 with LMAN1 in the context Chx A→B transcytosis. At 5 min post ILI of Chx266-hGH, a subset of the hGH[+] vesicles present in the apical region of enterocytes were also EEA1^{+} (Figure 6a). Simultaneously, LMAN1^{+} vesicles containing Chx266-hGH vesicles were observed within this same cellular location (Figure 6b). Co-localization of LMAN1 and EEA1 highlighted the extensive distribution of these proteins in the apical vesicular compartment relative to the basal region at this early stage of Chx A→B
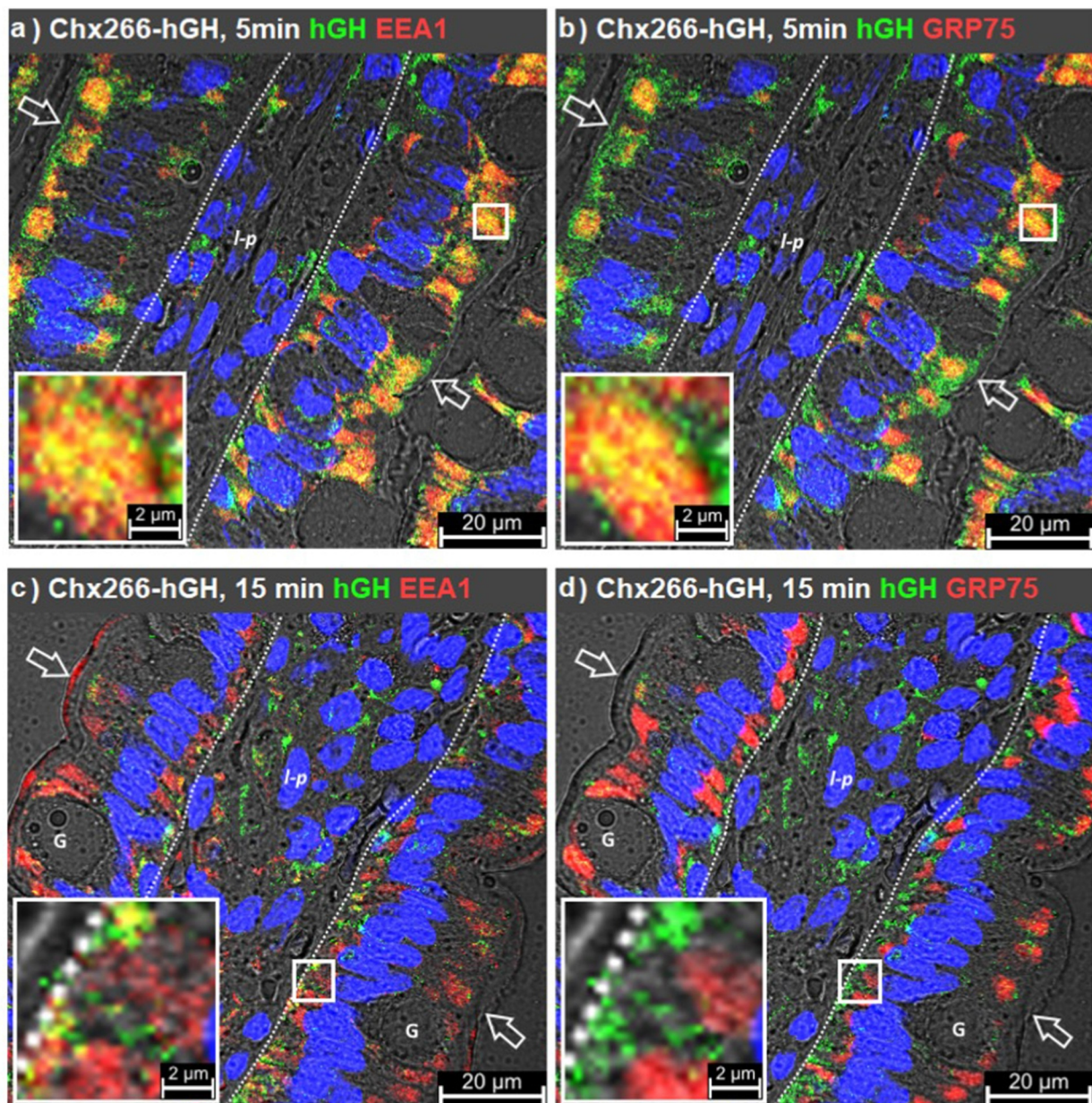
Figure 5. GRP75 does not associate with cholix in basal vesicular structures. Immunofluorescence microscopy was performed on rat jejunum after intraluminal injection (ILI) of Chx266-hGH. The human growth hormone (hGH) element of Chx266-hGH was co-localized with early endosomal antigen 1 (EEA1; a, c) or GRP75 (b, d) at 5- or 15-min post ILI. Apical (luminal) epithelial membrane (open arrow); basal epithelial cell surface-basement membrane demarcation (dashed line); *lamina propria* (*l-p*); goblet cell (g). Nuclei were stained with 4′,6-diamidino-2-phenylindole (DAPI; blue).

transcytosis (Figure 6c). Further, apical vesicles that contained EEA1 were observed in a subset of LMAN1$^+$ vesicles and were highly correlated with the distribution of vesicles that were EEA1$^+$/hGH$^+$ (Figure 6c). These results are consistent with a Chx A→B transcytosis process where the contents of EEA1$^+$ vesicles are delivered to LMAN1$^+$ vesicles in an apical vesicular sorting event.

A comparison of LMAN1 and GRP75 distributions at 15 min post ILI of Chx266-hGH was then performed to better understand the potential for GRP75 and LMAN1 to coordinate in the events of Chx A→B transcytosis. GRP75$^+$ vesicles showed a substantial overlap with Chx266-hGH in the apical vesicular compartment of enterocytes but again showed no co-localization in the basal region (Figure 6d). LMAN1$^+$ vesicles also showed a substantial overlap in the apical
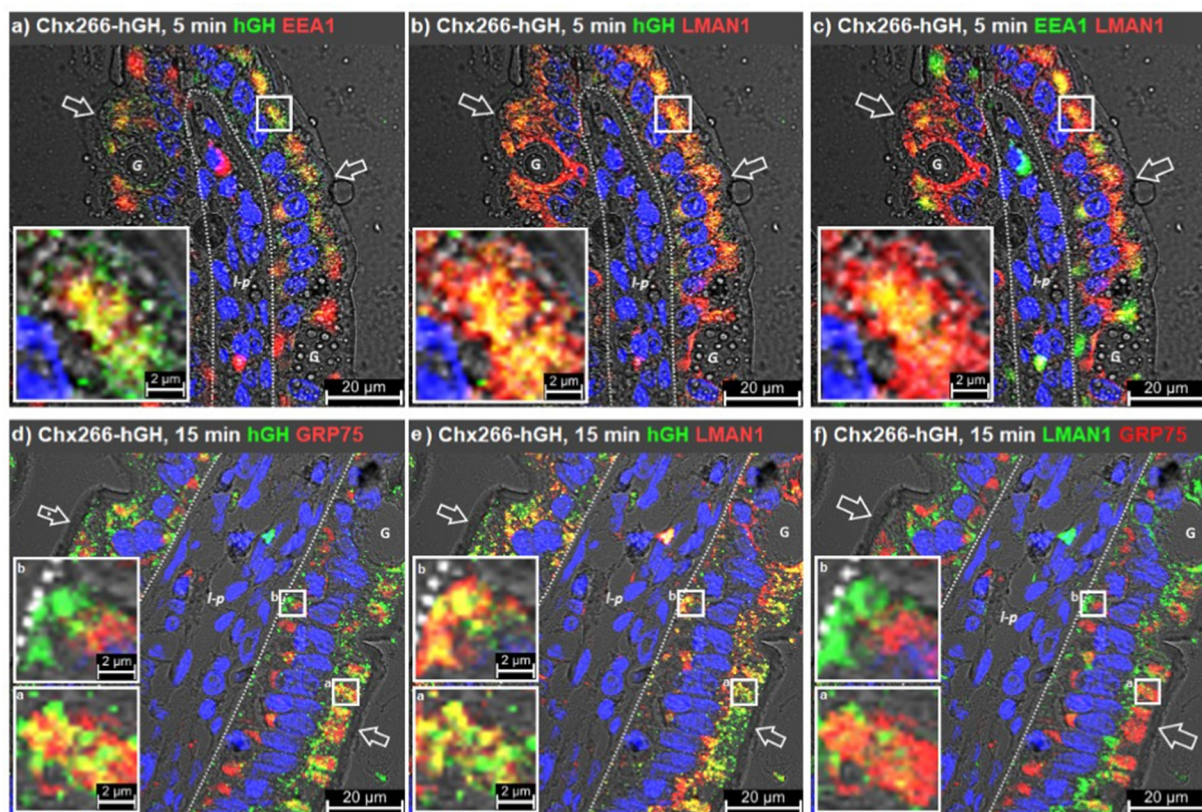
Figure 6. Cholix trafficking involves LMAN1-positive compartments. Immunofluorescence microscopy was performed on rat jejunum after intraluminal injection (ILI) of Chx266-hGH. The human growth hormone (hGH) element of Chx266-hGH was co-localized with a, early endosomal antigen 1 (EEA1) or b, LMAN1 at 5 min post ILI. c, Co-localization of EEA1 and LMAN1 at 5 min post ILI. Co-localization of hGH with d, GRP75 or e, LMAN1 at 15 min post ILI of Chx266-hGH. f, Co-localization of GRP75 and LMAN1 at 15 min post ILI of Chx266-hGH. Apical (luminal) epithelial membrane (open arrow); basal epithelial cell surface-basement membrane demarcation (dashed line); *lamina propria* (*l-p*); goblet cell (g). Nuclei were stained with 4',6-diamidino-2-phenylindole (DAPI; blue).

region with Chx266-hGH that was, unlike GRP75, carried over to the basal vesicular compartment of enterocytes (Figure 6e). Examination of apical vesicles that contained Chx266-hGH showed that some were GRP75^{+}, others were LMAN1^{+}, and some contained both GRP75 and LMAN1 (Figure 6d,e). Examination of GRP75 and LMAN1 distributions at 15 min post ILI of Chx266-hGH failed to demonstrate any notable co-localizations in either the apical or basal vesicular compartments. Such an organization for GRP75 and LMAN1 in hGH[+] apical vesicles would be consistent with this site providing a location for Chx transfer from GRP75 to LMAN1. Since Chx A→B transcytosis induces redistribution of LMAN1 from the apical to basal regions of enterocytes,[10] these data are consistent with Chx migration from GRP75 to LMAN1 in the apical vesicular region in an event that proceeds trafficking of the LMAN1-Chx complex to the basal vesicular region of the cell.

Chx trafficking involves apically positioned furin-positive compartments

Furin is a type I transmembrane protein that is primarily localized to the trans-Golgi network (TGN) but is not statically retained at that site and can traffic in local cycling loops as well as to the cell surface; differential processing of furin can direct it to the ERGIC, with the pro-peptide form functioning as an intracellular chaperone.[21] Further, furin has been shown to target to the basolateral surface of polarized epithelial cells.[22] Since these trafficking characteristics have similarities to those observed for Chx A→B transcytosis and to Chx transcytosis-mediated redistribution of LMAN1,[10] we examined the potential for furin to participate in Chx transcytosis.

At 15 minutes post ILI of Chx266-hGH, furin[+]/hGH[+] co-localizations were observed in the apical vesicular compartment with only very limited co-

localizations observed in the apical microvilli or the basal vesicular compartment of enterocytes (Figure 6a). Some furin[+]/hGH[+] co-localizations were noted in non-polarized cells within the lamina propria (Figure 7a). Examination of GRP75^{+}/hGH[+] co-localizations in these same tissues again showed restriction of these events to the apical vesicular compartment (Figure 7b). Furin[+]/GRP75^{+} co-localizations, however, were observed in the apical vesicular compartment to a far greater extent than in the basal vesicular compartment (Figure 7c). Sporadic furin[+]/hGH[+], but not furin[+]/GRP75^{+}, co-localizations were observed in enterocyte microvilli suggesting that the intersection of furin with the Chx A→B transcytosis pathway occurs prior to

engagement of GRP75, providing a possible mechanism for delivery of Chx to a furin[+]/ GRP75^{+} compartment soon after apical endocytosis.

We next examined the distribution of furin and LMAN1 during Chx A→B transcytosis to determine if, like LMAN1, furin redistributed in response to Chx endocytosis and/or its intracellular trafficking. As above, furin present in enterocyte microvilli showed occasional co-localizations with hGH at 15 min post ILI of Chx266-hGH (Figure 7d). Similarly, furin[+]/ hGH[+] vesicles were absent in the basal compartment, being restricted to the apical compartment (Figure 7d). Consistent with a previous report,[10]
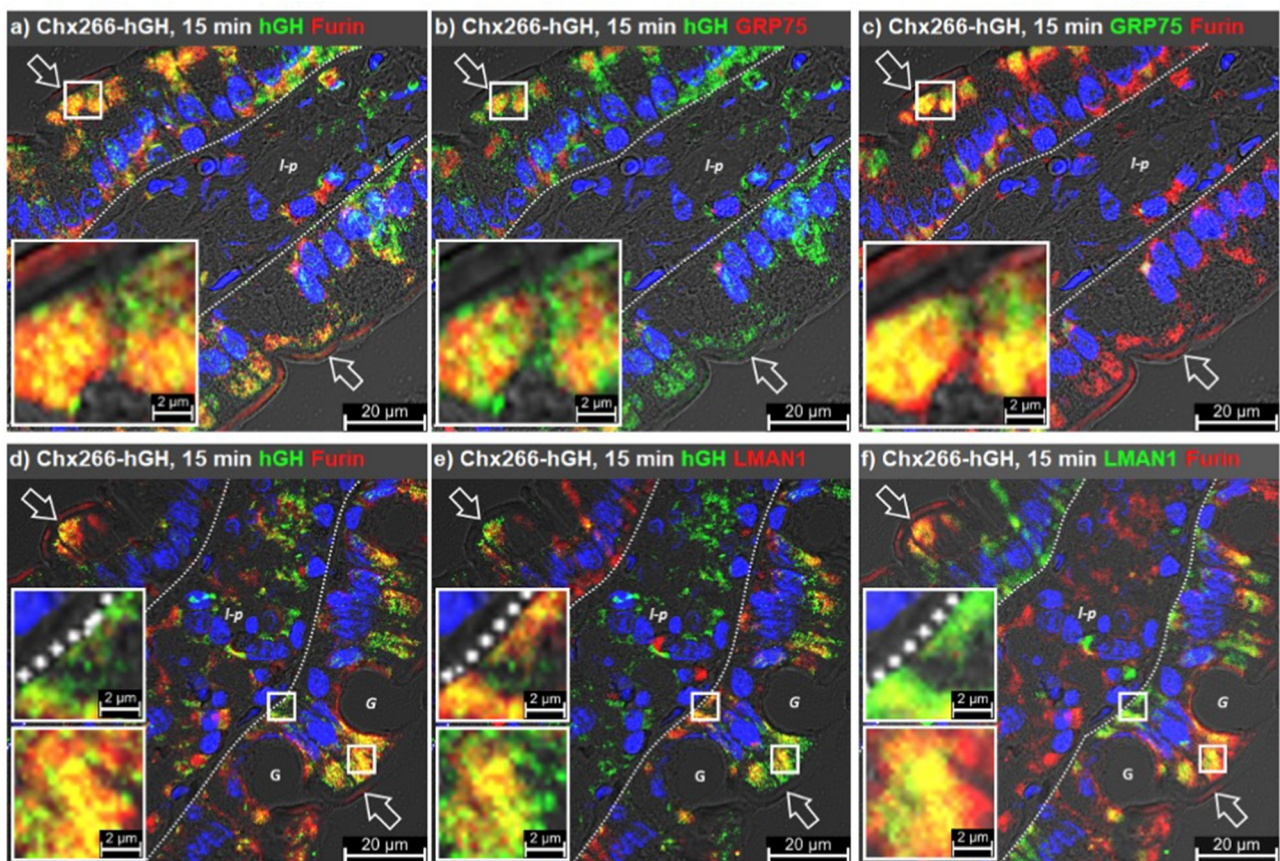

Figure 7. GRP75 intersects with furin differently than with LMAN1. Immunofluorescence microscopy was performed on rat jejunum after intraluminal injection (ILI) of Chx266-hGH. The human growth hormone (hGH) element of Chx266-hGH was co-localized with a, furin or b, GRP75 at 15 min post ILI. c, Co-localization of furin and GRP75 at 15 min post ILI. Co-localization of hGH with d, furin or e, LMAN1 at 15 min post ILI of Chx266-hGH. f, Co-localization of furin and LMAN1 at 15 min post ILI of Chx266-hGH. Apical (luminal) epithelial membrane (open arrow); basal epithelial cell surface-basement membrane demarcation (dashed line); *lamina propria* (*l-p*); goblet cell (g). Nuclei were stained with 4',6-diamidino-2-phenylindole (DAPI; blue).

LMAN1[+]/hGH[+] co-localizations were observed in both the apical and basal vesicular compartments (Figure 6e). Co-localization of LMAN1 and furin at 15 min post ILI of Chx266-hGH were more pronounced in the apical compared to the basal region of enterocytes (Figure 7f). While hGH[+]/LMAN1^{+}/furin[+] vesicles were observed in the apical vesicular compartment, this type of co-localization was not observed in the basal region of enterocytes (Figure 7d–f).

Characteristics of Chx interactions with GRP75 and other potential TRIPs

In an effort to better understand the basis for interactions between Chx and TRIPs potentially involved in its A→B transcytosis process, we evaluated binding of these proteins at three pH values to emulate the physiological environments of various cellular sites: the luminal surface at the time of apical endocytosis (LS; pH 7.4), the early endosome (EE; pH 6.3), and the late endosome (LE; pH 5.5).[23,24] While it is not possible to define the exact environmental conditions within the various vesicular compartments experienced by Chx during its A→B transcytosis, the intent was to determine relative levels of interaction for these Chx/TRIPs using an ELISA-type format where the specified pH was maintained for binding and wash steps. For these studies, we examined the potential for furin, TMEM132A, LMAN1, GRP75, or perlecan to associate with ntChx as a function of these three environmental conditions that are denoted by differences in pH (Figure 8a). Nonspecific interactions using bovine serum albumin were subtracted to correct for background variations in the assay. TMEM132A interacted comparably with ntChx under all three environmental conditions. Furin also interacted strongly at all three buffer pH conditions, with binding at pH 7.4 being slightly stronger relative to pH 6.3 and pH 5.5. LMAN1 interacted with ntChx in all three environmental conditions, but strongest at pH 5.5; GRP75 showed a similar pattern of interactions. Perlecan showed the strongest dependence on environmental conditions with pH 5.5 being preferred.

These data suggest that Chx can interact with a number of TRIPs during the A→B transcytosis process and that some of these interactions are dependent upon environmental conditions, providing potential hand-off mechanisms between specific TRIPs within discrete vesicle populations. To address the question of whether these potential Chx-TRIP interactions are competitive or independent, we performed a series of pull-down experiments (Figure 8b). All proteins used in these studies, performed at pH 7.4, were presented at equimolar levels that were projected to discriminate, at least at a crude level, competition from additive interactions with Chx. Magnetic beads coated with Chx266-hGH were capable of binding both TMEM132A and GRP75 proteins simultaneously, with the presence of TMEM132A possibly enhancing the extent of GRP75 binding. LMAN1 did not impede GRP75 binding under these conditions, while the presence of TMEM132A may have slightly enhanced LMAN1 binding to Chx266-hGH. Perlecan binding to Chx266-hGH was not affected by TMEM132A or GRP75 but seemed to be reduced by the presence of LMAN1. Such studies, however, do not examine the potential impact of environmental changes within endosomes that might drive Chx-TRIP interaction preferences and these events could be further amplified by vesicle migration within the cell, such as in the case of LMAN1 moving from apical to basal vesicular regions of the enterocyte and co-localization within specific cell regions. For example, here we show that interactions between Chx and GRP75 are restricted to the apical region of enterocytes, while interactions between Chx and perlecan were previously observed at both the apical and basal regions of enterocytes.[10]

Summary of Chx A→B transcytosis process

Putting GRP75/Chx interactions in the context of Chx A→B vesicular transcytosis, our studies have defined a putative pathway used by this exotoxin that involves a series of TRIPs. While not intended to define all elements involved in Chx A→B transcytosis, our data clarifies several events (Figure 9). 1) Chx endocytosis at the apical surface involves TMEM132A. 2) Chx interacts with furin in early endosome (EE) vesicles at a time when TMEM132A would recycle to the apical surface. 3) Chx moves with furin from EE to late endosome (LE) vesicles where it interacts with GRP75 and
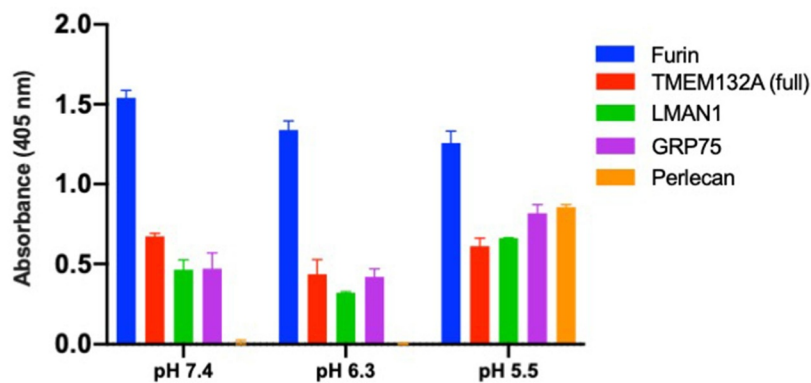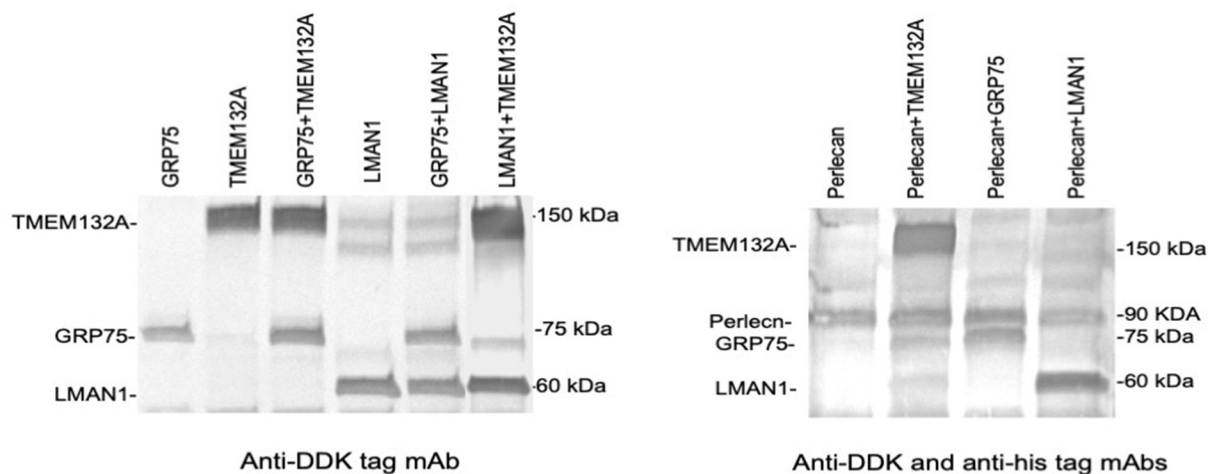
Figure 8. Interactions between Chx and co-localized proteins. a, ELISA-based studies where nontoxic, full length cholix (ntChx) was used to capture specific proteins under different pH and ionic conditions, with bovine serum albumin interactions being subtracted as a protein binding control. b, Western blots where Chx266-hGH attached to magnetic beads were used as bait at neutral pH to pull-down selected protein combinations.

potentially perlecan if there is a pH drop, events that would be consistent with these proteins directing Chx away from a lysosomal fate. 4) The ERGIC protein LMAN1 redistributes to the sorting endosome (SE) compartment in response to Chx endocytosis. 5) Chx-furin complexes in the SE move from GRP75 (and possibly perlecan as well) to LMAN1. 6) Chx-furin-LMAN1 traffics toward the supranuclear region of the cell. 7) Chx-LMAN1 traffics to the basal region of the cell without furin. 8) Chx-LMAN1 intersects with perlecan in a SE-like compartment where Chx is transferred to perlecan. 9) Perlecan then delivers Chx to the basal plasma membrane for exocytosis. 10) Perlecan engages with Chx delivered by LMAN1 via recycling endosome (RE) trafficking. 11) While present in the basal vesicular compartment, GRP75 and furin are not involved in Chx trafficking in this region of the cell. Our studies suggest that there are noncompetitive sites on Chx for its
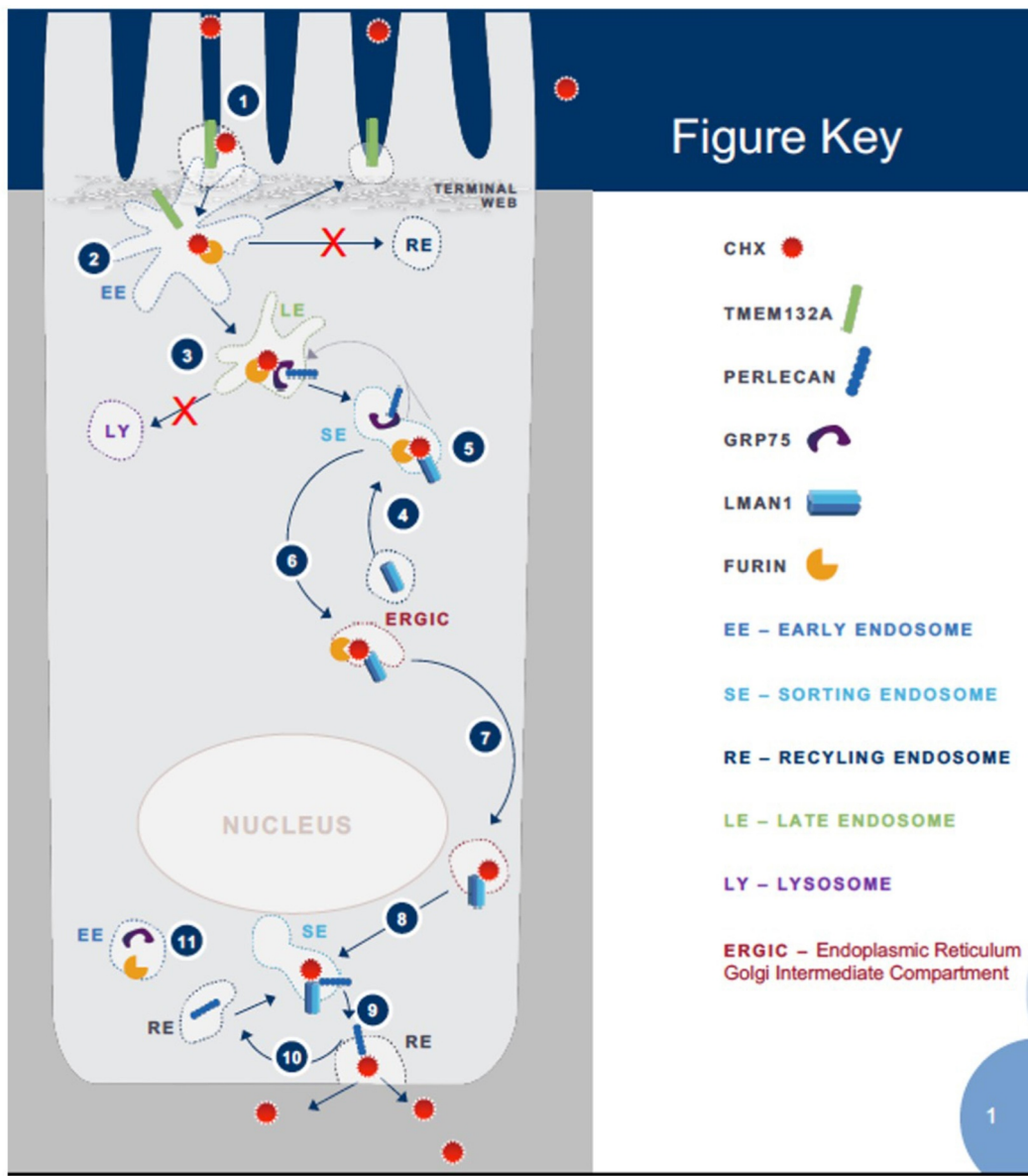
Figure 9. Diagram of events associated with cholix apical to basal transcytosis with interaction partners. Highlighted steps are explained in the text with greater detail. (1) Cholix enters at the apical plasma membrane in the microvilli area where it interacts with TMEM132A and furin. (2) Cholix enters an early endosomal compartment where it traffics preferentially to a late endosome rather than a recycling pathway. (3) Instead of continuing along the lysosomal degradation pathway, cholix interacts with GRP75 and moves to a sorting endosome. (4) Reorganization of LMAN1 from the endoplasmic reticulum intermediate Golgi complex (ERGIC) to apical sorting vesicles. (5) In this location, LMAN1 can intersect with cholix delivered to this site with furin and GRP75. (6) LMAN1 and furin appear to return with cholix to a supranuclear region of the cell consistent with location of the ERGIC. (7) Reorganization of LMAN1 from the ERGIC to the basal vesicular compartment provides a route for cholix to this region of the cell. (8) Cholix in complex with LMAN1 enters sorting endosomes in the basal vesicular compartment. (9) Within basal sorting endosomes, cholix/LMAN1 intersects with perlecan in a recycling endosome, which delivers it to the basal plasma membrane, resulting in cholix exocytosis and completion of the apical to basal transcytosis process. (10) Perlecan recycles to the basal sorting endosome where it can engage cholix trafficked to this site with LMAN1. (11) Unlike in the apical vesicular compartment, GRP75 and furin present in the basal vesicular compartment are not associated with cholix in this region of enterocytes.

interaction(s) with TMEM132A, GRP75, LMAN1, and perlecan, which could add to the efficiency of this A→B transcytosis process.

Discussion

A variety of bacterial toxins have acquired the capacity to overcome the tissue barrier presented by the intestinal epithelium. In some cases, these toxins efficiently overcome the barrier by damaging it: entering at the apical surface of polarized intestinal epithelial cells and gaining access to the host cell cytoplasm to exert their toxic actions from within epithelial cells to induce frank lesions.[1,25] Remarkably, the bacterial exotoxin Chx has the capacity to efficiently reach non-polarized cells in the lamina propria following its presentation at the apical surface using a vesicular transcytosis pathway that does not involve entering the cytoplasm of polarized intestinal epithelial cells.[16] Some aspects of the pathway used by Chx to achieve A→B vesicular transcytosis have been described, demonstrating the involvement of certain host cell proteins that function as TRIPs.[10] The current study expands the repertoire of known TRIPs used by Chx and defines a role for GRP75 that is restricted to interactions occurring in the apical vesicular compartment of polarized enterocytes. While GRP75 can be distributed in many locations within cells and has been shown to act in the cytoplasm to organize mitochondrial-endoplasmic reticulum Ca^{2+} signaling structures,[26,27] this heat shock protein has been identified as a functional constituent of non-caveolar, membrane raft-associated endocytic vesicles.[11] Here, we extend its vesicular role to include functioning as a TRIP for Chx A→B transcytosis in the apical location of enterocytes and with a timing consistent with limiting the delivery of Chx to lysosomes following apical endocytosis.

Chx uses an apical endocytosis event that involves TMEM132A and EEA1 to deliver it to early endosomes containing GRP75 in the apical compartment of enterocytes. Previous studies suggested a role for perlecan in its apical endocytosis and early trafficking,[10] with the current studies suggesting that this may involve a direct interaction with GRP75. Studies with non-polarized cells have demonstrated that perlecan can mediate a slower-than-expected pathway of internalization and

lysosomal delivery of a variety of ligands.[28] Specific interactions between perlecan and cell surface receptors, however, can also affect the fate of associated ligands following endocytosis, deviating their fate from the default outcome of routing to lysosomes.[29] In this polarized cell system, perlecan and GRP75 may function in routing Chx away from the default lysosomal degradation pathway,[30] facilitating the privileged pathway concept for the A→B transcytosis pathway hijacked by this exotoxin where it fails to enter lysosomes.[16] As GRP75 can interact with GRP94[31] and GRP94 appears to avoid lysosomes,[32] the mechanism used by Chx to avoid a lysosomal fate may involve the function of GRP75 binding partners.

Chx$^+$ apical vesicles containing both GRP75 and LMAN1 provide a potential site for transfer from the former to the latter. This presumed hand-off from GRP75 to LMAN1 would provide the mechanism that allows Chx to move from the apical vesicular region to the basal vesicular region of an enterocyte in coordination with the cellular redistribution of this ERGIC-associated protein that moves through the cell in COPII- and COPI-dependent processes;[33] COPII and COPI redistribute during Chx A→B transcytosis.[16] Our studies have also shown that while TMEM132A, GRP75, and perlecan fail to redistribute in response to apical Chx application, a second protein that redistributes was identified: furin. While LMAN1 started out only in the apical vesicular region, it was present in both the apical and basal vesicular regions following apical Chx application.[16] Furin was observed in a supranuclear region of enterocytes that would be consistent with the trans Golgi network (TGN) and apical Chx application resulted in furin movement to a more apical vesicular region of the cell and extensive co-localization with LMAN1. Movement of furin between the TGN and ERGIC compartments of cells can result from processing events associated with the chaperone function of this protease.[21,22]

While both furin and GRP75 were present in the basal vesicular region, Chx$^+$ vesicles in this part of the cell did not contain these TRIPs but did co-localize with LMAN1 as previously reported.[16] Even though Chx$^+$ vesicles in the apical region of enterocytes appear to contain both perlecan and LMAN1, Chx$^+$ vesicles in the basal region

contained either LMAN1 or perlecan, or both LMAN1 and perlecan.[16] These data emphasize the potential for LMAN1 to function as an intermediary trafficking element of Chx where it accepts the exotoxin in an apical compartment vesicle from GRP75 and delivers it to perlecan in a basal compartment. Since GRP75 and perlecan are present in both apical and basal vesicles, it is currently unclear how LMAN1, and its presumed client protein Chx, select between these two potential interaction and trafficking possibilities. A preference for pH-dependent interactions with Chx may provide at least a partial explanation for this selection process between GRP75 and perlecan. Importantly, Chx association with perlecan could lead to lysosomal degradation after internalization,[28] but this was not observed, suggesting that interaction and trafficking with LMAN1 was preferred. We have previously observed Chx$^+$ vesicles in the apical region are rab7$^+$, consistent with early-to-late endosomes, but that Chx$^+$ vesicles in the basal region are rab11a$^+$, consistent with a recycling population of endosomes.[16] Thus, there are potential local vesicle trafficking elements as well as modification to normal vesicle routing pathways that might be involved in this GRP75 versus perlecan selection process that discriminates regional LMAN1 interactions with Chx.

Previous intracellular trafficking studies of the family of bacterial exotoxins, that includes Chx, have described a pathway in non-polarized cells where proteolytic separation of toxin elements and routing to the cytoplasm are critical steps for their ability to reach the cytoplasm of these cells.[34] Such studies of Chx endocytosis in non-polarized cells demonstrated prohibitin 1 and 2 to be involved in intracellular trafficking events that ultimately targeted mitochondria;[35] it is interesting that we identify the mitochondrial heat shock protein GRP75 as a TRIP in our studies. Distinct entry pathway elements provide one potential explanation for the difference in cellular fate of Chx between non-polarized and polarized cells in the intestine. We noted TMEM132A to be involved in apical Chx endocytosis into polarized enterocytes and we failed to observe the expression of this protein on non-polarized cells within the lamina propria, although GRP75 was present in both cell populations.

In sum, the data presents a plausible process of successive TRIP engagement and release events that allows for apical endocytosis, apical to basal vesicular trafficking, and basal release that facilitates Chx passage from one TRIP (or TRIP complex) to another in a sequential fashion (Figure 8). Movement of Chx from one TRIP to another appears to involve both location within the cell and environmental (pH, ionic conditions, etc.) properties of the various vesicular compartments being accessed. It is intriguing that furin co-localizes with trafficking Chx, highlighting its function as a potential chaperone protein.[10,16] These studies also identify an additional cellular distribution (endosomes) and function (exotoxin trafficking) for GRP75 that already has been shown to have a plethora of actions from a variety of cellular locations.[36,37]

Materials and methods

Chx-related molecules

Non-toxin Chx (ntChx) was composed of full-length exotoxin containing a single E^{581}A mutation. Biotin-ntChx was prepared from the ntChx sequence being genetically fused at its C-terminus to a sequence that folded into a disulfide constrained short loop containing a tobacco etch virus protease cleavage sequence; reduction, protease cleavage, and chemical coupling to biotin was performed as previously described.[10] Chx266-hGH contained the first 266 amino acids of the exotoxin gene (Chx266) that was genetically fused to human growth hormone (hGH) through a polyglycine-serine-threonine (GS) spacer.[10] AMT-101 was composed of a genetic fusion through the GS linker between the first 386 amino acids of Chx (Chx386) and human interleukin 10. All proteins were prepared by standard protocols for *E. coli* expression following codon-optimization. Synthesized genes were cloned into the vector pET-26b (+) DNA expression vector and transformed into *E. coli* BL21(DE3) cells that were cultured by fed-batch fermentation in a stirred tank bioreactor using a defined culture media.[38] Cultures were induced with 1 mM IPTG and the temperature reduced to 26°C for a further 12 h after

induction before cells were harvested by centrifugation. Cell pellets were suspended in double distilled water, lysed using 2-passes of high-pressure using a microfluidizer, and clarified by centrifugation. Inclusion body pellets washed once with 50 mM Tris pH 8.5, 0.5 M NaCl, 20 mM ETDA, and once with double distilled water before solubilization in guanidine HCl, clarification by centrifugation, and dilution into refolding buffer that was gently mixed overnight. Refolded proteins were concentrated before buffer exchange by UF/DF into 25 mM Tris pH 7.5, 150 mM NaCl buffer loaded on a Capto Q ImpRes® anion exchange column, and then eluted using a NaCl gradient. A polishing step using ceramic hydroxyapatite Type I chromatography and an increasing linear sodium phosphate gradient was used to achieve further purification. Final protein concentration was assessed using A280, endotoxin was measured using Charles River Endosafe PTS reader, and purity (>90%) was assessed using SE-HPLC and SDS-PAGE.

Magnetic vesicle purification and protein identification by LC-MS/MS

Chemical conjugation of ntChx to 100 n diameter magnetic bead nanoparticles (Nanocs; New York, NY) to produced ntChx-MBNs was performed using a site- specific bioconjugation method.[39] Caco-2 cells were grown overnight to ~80% confluence, washed once with phosphate-buffered saline (PBS) and cultured in 6 mL of DMEM/F12 without FBS before addition of 0.5 mL of ntChx-MBNs in PBS. After incubation at 37°C for 1.5 hrs, cells were washed twice with PBS, collected by trypsin detachment, washed with PBS, and resuspended in 0.5 ml of PBS containing cOmplete™ mini protease inhibitor cocktail (Roche). Cells were disrupted mechanically on ice by passage through a 27-gauge needle, followed by the addition of $CaCl_2$ (final concentration 6 mM) and Benzonase (Fisher Science) and incubated for 20 min at 4°C. Remaining intact cells, cell debris, and nuclei were removed by centrifugation at 500 xg for 5 min. The resulting supernatant was pooled

with the supernatant obtained after a second centrifugation at 300 xg for 3 min. The supernatant was separated into a magnetic and nonmagnetic fraction using a magnetic separator (Promega).

For 2-D Western blotting, proteins of the pull-down samples from Caco-2 cell lysates using his-Chx-beads were separated on 2D DIGE gels with one CyDye Label and transferred onto membranes. Western blotting was performed using rabbit anti-human GRP75 as primary antibody followed by using Cy3-labeled Donkey anti-rabbit secondary antibody (Jackson ImmunoResearch, 1;2500). Western blot images were scanned using Typhoon 9400 (Applied Biomics, Hayward, CA). Proteins in non-magnetic and magnetic fractions were first resolved by 1D PAGE separation and then 2D DIGE analytical preparative gels.[40] Spots in magnetic fractions with high ratios in the DeCyder analysis were picked for protein identification by LC-MS/MS (Applied Biomics). Protein identification was based on peptide fingerprint mass mapping (MS data) and peptide fragmentation mapping (MS/MS data). MASCOT software was used to search engine to identify proteins from primary sequence databases.

Cholix and GRP75 pull-down and co-immunoprecipitation assays

Invitrogen systems were used for pulldowns involving hexa-histidine (H_6)-tagged proteins (catalog # 10103D) or biotin-streptavidin using Dynabeads M-280 (catalog # 11205D). Full-length ntChx protein with a C-terminal cys-TEV-cys-H_6 sequence was used before or after biotin addition.[10] Caco-2 cell lysate were prepared in RIPA lysis buffer (Invitrogen, # 89900). Lysates (0.5 mL; 100 μg) were incubated with ntChx (H_6 or biotin) protein (10 μg) with slight agitation overnight at 4 °C and then incubated with anti-Chx polyclonal or anti-GRP75 monoclonal antibodies coupled to 2.8 μm diameter magnetic beads using Dynabead Co-IP kit (Invitrogen, # 14321D) for 3 h at 4 °C. Rabbit IgG was used as a negative control. Immune complexes were collected by magnetic separator (Promega), with the pellet being washed five times with cold

PBS containing cOmplete™ mini protease inhibitor cocktail (Roche). Proteins in the pellet were subjected to immunoblotting analysis.

ELISA-based studies

96-well Costar plates (Corning, Corning Life Sciences B.V., Amsterdam, The Netherlands) were coated with ntChx and blocked with 3% BSA. Potential interacting molecules were added, following dilution into 3% BSA, to wells and incubated for 1 h at RT. Captured ntChx-TRIPs events were detected using specific antibodies in an ELISA microplate reader format where detection was determined by enzymatic reactions read at 405 nm (Bio-Rad). For interactions between GRP75 or other HSPs and ntChx, 96-well Costar plates were coated with ntChx or potential interacting molecule PBS. After blocking with 3%BSA, GRP75 or other HSPs were added to wells and incubated for 1 h at RT. The captured HSPs were detected using a specific anti-HSP Ab. Interaction studies using were performed similarly for Chx266-hGH or an equal molar concentration of hGH (to serve as a control) in PBS. Wells were blocked in 3% BSA. Flag-tag-labeled versions of test proteins (Origene Technologies, Inc., Rockville, MD) at 2 μg/ml in 3% BSA (pH 5.5 or pH 7.5) were then incubated for 1 h at RT. Wells coated with 3% BSA without proteins served as an additional control. The captured test proteins were detected using anti-Flag mAb (Origene Technologies, Inc). All ELISA plates were run in triplicate.

Stable knockdown in Caco-2 cells and invitro transport

Caco-2 cells (ATCC HTB-37) were maintained in DMEM supplemented with 10% heat inactivated fetal bovine serum (Hyclone SH30070.03IR), 1x L-glutamine (ATCC), 1x Pen/Strep (VWR #97063-708), and 1x non-essential amino acids. Cells were sub-cultured when they were about 80% confluent. Disruption of the human gene grp75 (HSPA9) in Caco-2 cells was carried out using a HDR-mediated CRISPR/Cas9 kit (KN201397, OriGene Technologies, Rockville, MD, USA). Stable cells where the grp75 gene was disrupted were selected with puromycin. Extent of protein down regulation was determined using Western blotting and ImageJ software.

For *in vitro* transport experiments, Caco-2 cells (1.5×10^5 cells/mL in 0.5 mL medium) were seeded onto 0.4 μm pore size inserts (Corning Cat. # 3401) and 1.5 ml of medium was added per basal well. Culture medium was exchanged every 2 days until day 21 when functionally tight monolayers were formed as assessed by trans-epithelial electrical resistance > 500 $\Omega \bullet cm^2$ and 70 kDa dextran transport was not observed. Inserts were washed once with PBS before the addition of Chx266-hGH (20 μg/mL in 100 μL) or the control protein hGH at an equimolar amount to the apical surface and 500 μL of PBS to basolateral chamber. After incubation at 37°C for 60 min, basolateral solutions were collected for transport analysis using.

For Western blotting to assess *in vitro* transcytosis, samples were separated by electrophoresis in a 4–12% NuPAGE gel (BioRad) prior to transfer onto a PVDF membrane (BioRad). Bands were probed with a goat anti-hGH (R&D Systems), followed by AP-conjugated secondary rabbit anti-goat antibody (Abcam) and visualized using an AP Western blotting substrate (Promega). Inhibition of Chx *in vitro* transport by anti-GRP75 or anti-perlecan antibodies was performed by pre-mixing 20 μg/mL antibody with 20 μg/mL Chx266-hGH in 100 μL PBS prior to apical surface application. An isotype antibody recognizing human IL-10 was used as a control. Transported Chx266-hGH in the basal media was analyzed after incubation at 37°C for 60 min. All experiments were performed in triplicate.

In vivo *transcytosis*

Male Wistar rats, housed 3–5 per cage with a 12/12 h light/dark cycle, were 225–275 g (approximately 6–8 weeks old) when placed on study. All experiments were conducted during the light phase using a non-recovery protocol that used continuous isoflurane anesthesia. A 4–5 cm midline abdominal incision exposed mid-jejunum regions. Stock solutions at 3.86×10^{-5} M of test articles were prepared in PBS, with 50 μL (per 250 g rat) being administered by intraluminal injection (ILI) using a 29-gauge needle. The injection site mesentery was marked with

a permanent marker. At study termination, a 3–5 mm region that captured the marked intestine segment was isolated and processed for microscopic assessment. All experiments were performed in accordance with the U.K. Animals (Scientific Procedures) Act of 1986, the European Communities Council Directive of 1986 (86/609/EEC), and the University of Bath's ethical review procedures.

Immunofluorescence microscopy

Isolated intestinal tissues were fixed in 4% paraformaldehyde at 4°C for 18–24 h, processed using a Leica TP1020 tissue processor, dehydrated in increasing concentrations of ethanol, cleared with HistoClear (National Diagnostics), and infused with molten paraffin wax. Sections cut from tissue-embedded paraffin wax blocks (5 μm thickness; Jung Biocut2035 microtome) were mounted on glass microscope slides, rehydrated, and processed for antigen retrieval by boiling slides in 10 mM sodium citrate for 10 min followed by washing with PBS. Processed tissue slices were permeabilized using 0.1% Triton X-100 in PBS for 30 min, blocked using 2% donkey or goat serum and 2% BSA in 0.1% Triton X-100 in PBS for 2 h, and incubated overnight at 4°C with primary antibodies diluted in 1% BSA and 0.05% Triton X-100 in PBS at 4°C. Tissue slices were washed thrice with PBS, incubated for 2 h with secondary antibodies conjugated to AlexaFluor® fluorescent dyes, washed thrice with PBS, and incubated for 1 h in 200 nM DAPI, washed with PBS, dehydrated in ethanol, and covered by mounting a coverslip with Fluorshield (Abcam) mounting media; all steps performed at room temperature unless otherwise noted. After allowing the mounting media to dry at 4°C overnight, fluorescent images were obtained using a Zeiss 880 LSM confocal microscope, a Perkin Elmer Vectra, or a Leica SP5 inverted confocal microscope using the following settings. Excitation/emission wavelengths used for the various fluorophores were: DAPI (405 nm/462 nm), Alexafluor 488 (488 nm/562 nm), Alexafluor 564 (561 nm/602 nm), and Alexafluor 633 (633 nm/693 nm). The pinhole was set between 0.99 and 1.22 airy units to achieve a z-resolution of 0.8 μm. All laser intensities were set at 2%. All images were captured with a total magnification of 100X-630X. Image analytics software included Zeiss Zen 2.6 Blue software, Leica SP5, Perkin Elmer Phenochart and Inform, Imaris, and ImageJ.

Antibodies and recombinant proteins

Primary antibodies: Mouse anti-GRP75 mAb (Abcam, ab2799); mouse anti-hsp60 mAb (Abcam, ab110312); mouse anti-GRP78 mAb (Abcam, ab25192); mouse anti-Hsp90 mAb (Abcam, ab79849); mouse anti-HSPG mAb (Abcam, ab23418); rabbit anti-DKK1 pAb (Abcam, ab61034); rabbit anti-cytokeratin 1 pAb (Abcam, ab93652); rabbit anti-cytokeratin 8 pAb (Abcam, ab154301); mouse anti-DDK/FLAG mAb (Origene, TA150030); goat anti-human growth pAb (R&D Systems, AF1067); mouse anti-IL22 mAb (Abcam, ab134035); rabbit anti-Chx antibodies (prepared in house at AMT); mouse anti-EEA1 mAb (Abcam, ab70521).

Secondary antibodies: Goat anti-rabbit IgG H&L conjugated with Alkaline Phosphatase (AP) (Abcam, ab97048); rabbit anti-goat IgG H&L (AP) (Abcam, ab6742); rabbit anti-mouse IgG (H + L) (AP) (Jackson ImmunoResearch, 315-055-003); donkey anti-rabbit IgG antibody (Peroxidase) (Jackson ImmunoResearch, 711-035-152); donkey anti-mouse IgG antibody (peroxidase) (Jackson ImmunoResearch, 715-035-150); Cy3- and Cy5-labeled donkey anti-mouse IgG (Jackson ImmunoResearch,715-165-151, 715-175-150,); donkey anti-rabbit IgG-aleafluore546 (Invitrogen, A10040); donkey anti-goat-IgG-alexafluore488 (Invitrogen, A11055).

Recombinant Proteins: Chx and Chx266-hGH proteins were expressed and purified (prepared in house at AMT) as previously described.[10] ntChx was produced as a fusion protein with biotin at its Cterminus. Other recombinant proteins: GRP75 (ab115711), Keratin 1 (ab114282), keratin 8 (ab156970), was purchased from Abcam. HSPG, LMAN1, TMEM132A, HSP60, HSP78, HSP90 were purchased from Origene.

Disclosure statement

ORCID

Alistair Taverner 🔾 http://orcid.org/0000-0002-2507-8694
Randall J. Mrsny 🔾 http://orcid.org/0000-0001-8505-8516

Highlights

(1) A screen for proteins associated with cholix (Chx) transcytosis identified GRP75; specific interactive/functional properties were validated in binding and knock-down studies.
(2) Chx transiently interacts with GRP75 primarily in an apical vesicular endosomal compartment involved in epithelial cell transcytosis, limiting recycling or degradation outcomes.
(3) The intravascular role of GRP75 interactions represent one of several elements identified for Chx trafficking events following apical endocytosis that leads to transcytosis.

References

1. Williams JM, Tsai B. Intracellular trafficking of bacterial toxins. Curr Opin Cell Biol. 2016;41:51–56. doi:10.1016/j.ceb.2016.03.019.
2. Ahmed W, Zheng K, Liu ZF. Establishment of chronic infection: Brucella's stealth strategy. Front Cell Infect Microbiol. 2016;6:30. doi:10.3389/fcimb.2016.00030.
3. Lemichez E, Barbieri JT. General aspects and recent advances on bacterial protein toxins. Cold Spring Harb Perspect Med. 2013;3(2):a013573. doi:10.1101/cshperspect.a013573.
4. Henkel JS, Baldwin MR, Barbieri JT. Toxins from bacteria. EXS. 2010;100:1–29. doi:10.1007/978-3-7643-8338-1_1.
5. Mrsny RJ. Lessons from nature: "Pathogen-Mimetic" systems for mucosal nano-medicines. Adv Drug Deliv Rev. 2009;61(2):172–192. doi:10.1016/j.addr.2008.09.009.
6. Lucas R, Hadizamani Y, Gonzales J, Gorshkov B, Bodmer T, Berthiaume Y, Moehrlen U, Lode H, Huwer H, Hudel M, et al. Impact of bacterial toxins in the lungs. Toxins (Basel). 2020;12(4):223. doi:10.3390/toxins12040223.
7. Awasthi SP, Asakura M, Chowdhury N, Neogi SB, Hinenoya A, Golbar HM, Yamate J, Arakawa E, Tada T, Ramamurthy T, et al. Novel cholix toxin variants, ADP-ribosylating toxins in Vibrio cholerae non-O1/non-O139 strains, and their pathogenicity. Infect Immun. 2013;81(2):531–541. doi:10.1128/IAI.00982-12.
8. Fieldhouse RJ, Jorgensen R, Lugo MR, Merrill AR. The 1.8 A cholix toxin crystal structure in complex with NAD+ and evidence for a new kinetic model. J Biol Chem. 2012;287(25):21176–21188. doi:10.1074/jbc.M111.337311.
9. Jorgensen R, Purdy AE, Fieldhouse RJ, Kimber MS, Bartlett DH, Merrill AR. Cholix toxin, a novel ADP-ribosylating factor from Vibrio cholerae. J Biol Chem. 2008;283(16):10671–10678. doi:10.1074/jbc.M710008200.
10. Taverner A, MacKay J, Laurent F, Hunter T, Liu K, Mangat K, Song L, Seto E, Postlethwaite S, Alam A, et al. Cholix protein domain I functions as a carrier element for efficient apical to basal epithelial transcytosis. Tissue Barriers. 2020;8(1):1710429. doi:10.1080/21688370.2019.1710429.
11. Wittrup A, Zhang S-H, Svensson KJ, Kucharzewska P, Johansson MC, Morgelin M, Belting M. Magnetic nanoparticle-based isolation of endocytic vesicles reveals a role of the heat shock protein GRP75 in macromolecular delivery. Proc Natl Acad Sci U S A. 2010;107(30):13342–13347. doi:10.1073/pnas.1002622107.
12. Nava-Acosta R, Navarro-Garcia F, Sperandio V, Zychlinsky A. Cytokeratin 8 is an epithelial cell receptor for pet, a cytotoxic serine protease autotransporter of enterobacteriaceae. mBio. 2013;4(6):e00838–00813. doi:10.1128/mBio.00838-13.
13. Oh-hashi K, Naruse Y, Amaya F, Shimosato G, Tanaka M. Cloning and characterization of a novel GRP78-binding protein in the rat brain. J Biol Chem. 2003;278(12):10531–10537. doi:10.1074/jbc.M212083200.
14. Li B, Niswander LA. TMEM132A, a novel wnt signaling pathway regulator through wntless (WLS) interaction. Front Cell Dev Biol. 2020;8:599890. doi:10.3389/fcell.2020.599890.
15. Sanchez-Pulido L, Ponting CP, Kelso J. TMEM132: an ancient architecture of cohesin and immunoglobulin domains define a new family of neural adhesion molecules. Bioinformatics. 2018;34(5):721–724. doi:10.1093/bioinformatics/btx689.
16. Fay NC, Muthusamy B-P, Nyugen LP, Desai RC, Taverner A, MacKay J, Seung M, Hunter T, Liu K, Chandalia A, et al. A novel fusion of IL-10 engineered to traffic across intestinal epithelium to treat colitis. J Immunol. 2020;205(11):3191–3204. doi:10.4049/jimmunol.2000848.
17. Beer AJ, Gonzalez Delgado J, Steiniger F, Qualmann B, Kessels MM. The actin nucleator Cobl organises the terminal web of enterocytes. Sci Rep. 2020;10(1):11156. doi:10.1038/s41598-020-66111-9.
18. Hull BE, Staehelin LA. The terminal web. A reevaluation of its structure and function. J Cell Biol. 1979;81(1):67–82. doi:10.1083/jcb.81.1.67.

19. Hirokawa N, Tilney LG, Fujiwara K, Heuser JE. Organization of actin, myosin, and intermediate filaments in the brush border of intestinal epithelial cells. J Cell Biol. 1982;94(2):425–443. doi:10.1083/jcb.94.2.425.

20. Wilson JM, de Hoop M, Zorzi N, Toh B-H, Dotti CG, Parton RG. EEA1, a tethering protein of the early sorting endosome, shows a polarized distribution in hippocampal neurons, epithelial cells, and fibroblasts. Mol Biol Cell. 2000;11(8):2657–2671. doi:10.1091/mbc.11.8.2657.

21. Anderson ED, Molloy SS, Jean F, Fei H, Shimamura S, Thomas G. The ordered and compartment-specfific autoproteolytic removal of the furin intramolecular chaperone is required for enzyme activation. J Biol Chem. 2002;277(15):12879–12890. doi:10.1074/jbc.M108740200.

22. Thomas G. Furin at the cutting edge: from protein traffic to embryogenesis and disease. Nat Rev Mol Cell Biol. 2002;3(10):753–766. doi:10.1038/nrm934.

23. Scott CC, Gruenberg J. Ion flux and the function of endosomes and lysosomes: pH is just the start: the flux of ions across endosomal membranes influences endosome function not only through regulation of the luminal pH. Bioessays. 2011;33(2):103–110. doi:10.1002/bies.201000108.

24. Scott CC, Vacca F, Gruenberg J. Endosome maturation, transport and functions. Semin Cell Dev Biol. 2014;31:2–10. doi:10.1016/j.semcdb.2014.03.034.

25. Watson P, Spooner RA. Toxin entry and trafficking in mammalian cells. Adv Drug Deliv Rev. 2006;58(15):1581–1596. doi:10.1016/j.addr.2006.09.016.

26. D'Eletto M, Rossin F, Occhigrossi L, Farrace MG, Faccenda D, Desai R, Marchi S, Refolo G, Falasca L, Antonioli M, et al. Transglutaminase type 2 regulates ER-mitochondria contact sites by interacting with GRP75. Cell Rep. 2018;25(13):3573–3581 e3574. doi:10.1016/j.celrep.2018.11.094.

27. Wadhwa R, Takano S, Kaur K, Aida S, Yaguchi T, Kaul Z, Hirano T, Taira K, Kaul S. Identification and characterization of molecular interactions between mortalin/mtHsp70 and HSP60. Biochem J. 2005;391(2):185–190. doi:10.1042/BJ20050861.

28. Fuki IV, Iozzo RV, Williams KJ. Perlecan heparan sulfate proteoglycan: a novel receptor that mediates a distinct pathway for ligand catabolism. J Biol Chem. 2000;275(33):25742–25750. doi:10.1074/jbc.M909173199.

29. Belting M. Heparan sulfate proteoglycan as a plasma membrane carrier. Trends Biochem Sci. 2003;28(3):145–151. doi:10.1016/S0968-0004(03)00031-8.

30. Cullen PJ, Steinberg F. To degrade or not to degrade: mechanisms and significance of endocytic recycling. Nat Rev Mol Cell Biol. 2018;19(11):679–696. doi:10.1038/s41580-018-0053-7.

31. Takano S, Wadhwa R, Mitsui Y, Kaul SC. Identification and characterization of molecular interactions between glucose-regulated proteins (GRPs) mortalin/GRP75/peptide-binding protein 74 (PBP74) and GRP94. Biochem J. 2001;357(2):393–398. doi:10.1042/bj3570393.

32. Wassenberg JJ, Dezfulian C, Nicchitta CV. Receptor mediated and fluid phase pathways for internalization of the ER Hsp90 chaperone GRP94 in murine macrophages. J Cell Sci. 1999;112(Pt 13):2167–2175. doi:10.1242/jcs.112.13.2167.

33. Fu YL, Zhang B, Mu TW. LMAN1 (ERGIC-53) promotes trafficking of neuroreceptors. Biochem Biophys Res Commun. 2019;511(2):356–362. doi:10.1016/j.bbrc.2019.02.053.

34. Smith DC, Spooner RA, Watson PD, Murray JL, Hodge TW, Amessou M, Johannes L, Lord JM, Roberts LM. Internalized pseudomonas exotoxin A can exploit multiple pathways to reach the endoplasmic reticulum. Traffic. 2006;7(4):379–393. doi:10.1111/j.1600-0854.2006.00391.x.

35. Yahiro K, Ogura K, Terasaki Y, Satoh M, Miyagi S, Terasaki M, Yamasaki E, Moss J. Cholix toxin, an eukaryotic elongation factor 2 ADP-ribosyltransferase, interacts with prohibitins and induces apoptosis with mitochondrial dysfunction in human hepatocytes. Cell Microbiol. 2019;21(8):e13033. doi:10.1111/cmi.13033.

36. Flachbartova Z, Kovacech B. Mortalin - a multipotent chaperone regulating cellular processes ranging from viral infection to neurodegeneration. Acta Virol. 2013;57:3–15. doi:10.4149/av_2013_01_3.

37. Wadhwa R, Taira K, Kaul SC. An Hsp70 family chaperone, mortalin/mthsp70/PBP74/Grp75: what, when, and where? Cell Stress Chaperones. 2002;7(3):309–316. doi:10.1379/1466-1268(2002)007<0309:AHFCMM>2.0.CO;2.

38. Korz DJ, Rinas U, Hellmuth K, Sanders EA, Deckwer WD. Simple fed-batch technique for high cell density cultivation of Escherichia coli. J Biotechnol. 1995;39(1):59–65. doi:10.1016/0168-1656(94)00143-Z.

39. Chen D, Disotuar MM, Xiong X, Wang Y, Chou DH. Selective N-terminal functionalization of native peptides and proteins. Chem Sci. 2017;8(4):2717–2722. doi:10.1039/C6SC04744K.

40. Pasquali M, Serchi T, Planchon S, Renaut J. 2D-DIGE in proteomics. Methods Mol Biol. 2017;1654:245–254.